

Research Article

Synthesis, Spectroscopic, and Thermal Investigations of Metal Complexes with Mefenamic Acid

Karolina Kafarska, Michał Gacki, and Wojciech M. Wolf

*Institute of General and Ecological Chemistry, Faculty of Chemistry, Lodz University of Technology,
116 Zeromskiego Street, 90-924 Lodz, Poland*

Correspondence should be addressed to Karolina Kafarska; karolina.kafarska@p.lodz.pl

Received 18 September 2017; Revised 16 November 2017; Accepted 21 November 2017; Published 18 December 2017

Academic Editor: Maria F. Carvalho

Copyright © 2017 Karolina Kafarska et al. This is an open access article distributed under the Creative Commons Attribution License, which permits unrestricted use, distribution, and reproduction in any medium, provided the original work is properly cited.

The novel metal complexes with empirical formulae $M(\text{mef})_2 \cdot n\text{H}_2\text{O}$ (where $M = \text{Mn(II)}, \text{Co(II)}, \text{Ni(II)}, \text{Cu(II)}, \text{Zn(II)},$ and Cd(II) ; *mef* is the mefenamic ligand) were synthesized and characterized by elemental analysis, molar conductance, FTIR-spectroscopy, and thermal decomposition techniques. All IR spectra revealed absorption bands related to the asymmetric (ν_{as}) and symmetric (ν_{s}) vibrations of carboxylate group. The Nakamoto criteria clearly indicate that this group is bonded in a bidentate chelate mode. The thermal behavior of complexes was studied by TGA methods under non-isothermal condition in air. Upon heating, all compounds decompose progressively to metal oxides, which are the final products of pyrolysis. Cu(II) , Zn(II) , and Cd(II) complexes were also characterized by the coupled TG-FTIR technique, which finally proved the path and gaseous products of thermal decomposition. Additionally, the coupled TG-MS system was used to determine the principal volatile products of thermolysis and fragmentation processes of $\text{Mn}(\text{mef})_2 \cdot 3\text{H}_2\text{O}$ and $\text{Co}(\text{mef})_2 \cdot 2\text{H}_2\text{O}$.

1. Introduction

Fenemates (N-arylated derivatives of anthranilic acid) are pharmaceutical compounds with distinct anti-inflammatory and analgesic, antipyretic activity. Their mode of biological action is based on inhibiting prostaglandin synthetase [1, 2]. In particular, 2-(2,3-dimethyl-phenyl) aminobenzoic acid (mefenamic acid: $(\text{CH}_3)_2\text{C}_5\text{H}_3\text{NHC}_5\text{H}_4\text{COOH}$ (Figure 1)) is an effective nonsteroidal agent widely used for the treatment of mild to moderate pains, inflammation, ache, and fever [3–5]. Moreover mefenamic acid, as other anti-inflammatory drugs, is emerging as novel chemopreventive agents against cancer [6, 7]. It is an active ingredient of numerous drugs which are present on the pharmaceutical market [8, 9]. However, NSAID-induced side effects, particularly in the gastrointestinal tract and kidney, often limit their applications. For this reason, considerable efforts have been made to increase their activity while minimizing side effects [10].

It is well known that several transition metal complexes with nonsteroidal drugs are more effective and show significantly lower toxicity than that of their parent drugs [11, 12]. In

particular, divalent metal complexes with several NSAID are better anti-inflammatory candidates than NSAIDs, because they have unique structures that could interact with the target enzymes more specifically. In addition, metal ions introduce extra antioxidant activity [13] and antiproliferative activity against cancer [14–16]. Furthermore gastrointestinal toxicities associated with the administration of complexes are much lower than those of the parent drug and improved safety of these drugs [17].

Our studies were stimulated by the fact that majority of anti-inflammatory drugs are carboxylic acids with their carboxylate group prone to metal binding [11, 18–20]. Some of mefenamate complexes have been described in the literature. Brzyska and Ożga characterized complexes of rare earth metals with mefenamic ligand [21]. Tapacli and Ide described mefenamate compounds with Ca and Na ions [22]. Kovala-Demertzi et al. investigated the compounds with the formulae: $\text{SnPh}_3(\text{mef})$ and $\text{SnBu}_2(\text{mef})_2$ [23].

The aim of the present work was to obtain the mefenamate complexes of Mn(II) , Co(II) , Ni(II) , Cu(II) , Zn(II) , and

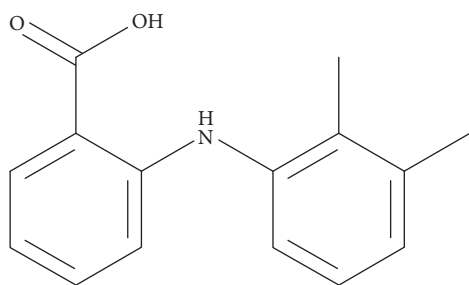


FIGURE 1: Chemical structure of mefenamic acid.

Cd(II), determine their chemical properties, and study their thermal decomposition patterns.

2. Materials and Methods

2.1. Materials. Pure mefenamic acid was obtained as a gift from Polfa Pabianice; metal chlorides $MCl_2 \cdot nH_2O$ (where $M = Mn, Co, Ni, Cu, Zn,$ and Cd), DMSO, DMF, and EtOH p.a. were purchased from Aldrich and MeOH from Lab-Scan; other chemicals were from POCh-Gliwice.

2.2. Synthesis. All complexes were obtained according to similar procedures. The first step of synthesis was preparation sodium salt of ligand by dissolution of mefenamic (1 mmol) acid in 50 mL fresh precipitated aqueous-ethanol solution (1:1) of NaOH ($0,02 \text{ mol} \cdot \text{L}^{-1}$). The mixture was heated up to 60°C and added to aqueous solution of metal chlorides ($0,5 \text{ mol}$ in 25 mL). The reaction mixture was kept in 60°C for 2 hours. After several days the solid precipitates were isolated by filtration, washed with hot water, and dried on air.

Complex $Mn(mef)_2 \cdot 3H_2O$: color: pale pink; IR (KBr, ν): 3358 (OH), 3067 (NH), 2859 (CH), 1652 (NH), 1578 (OCO^-), 1495 (NH), 1459 (CH_3), 1394 (OCO^-), 1283 (CH_3), 1183 (CH_3), 1159 (CH), 1093 (CH), 1043 (CH_3), 852 (CH), 749 (CH_3), 679 (MO) cm^{-1} ; Anal. Calc. $C_{30}H_{34}MnN_2O_7$ (%): C, 61.12; H, 5.81; N, 4.75; Mn, 9.32; Found (%): C, 61.00; H, 5.50; N, 4.76; Mn, 9.36.

Complex $Co(mef)_2 \cdot 2H_2O$: color: pink; IR (KBr, ν): 3315 (OH), 3069 (NH), 1651 (NH), 1578 (OCO^-), 1504 (NH), 1454 (CH_3), 1393 (OCO^-), 1283 (CH_3), 1188 (CH_3), 1159 (CH), 1097 (CH), 1043 (CH_3), 854 (CH), 748 (CH_3), 675 (MO) cm^{-1} ; Anal. Calc. $C_{30}H_{32}CoN_2O_6$ (%): C, 62.61; H, 5.60; N, 4.87; Co, 10.24; Found (%): C, 62.67; H, 5.60; N, 4.88; Co, 10.22.

Complex $Ni(mef)_2 \cdot 2H_2O$: color: pale green; IR (KBr, ν): 3346 (OH), 3069 (NH), 2860 (CH), 1653 (NH), 1578 (OCO^-), 1499 (NH), 1455 (CH_3), 1391 (OCO^-), 1285 (CH_3), 1190 (CH_3), 1159 (CH), 1097 (CH), 1043 (CH_3), 851 (CH), 748 (CH_3), 678 (MO) cm^{-1} ; Anal. Calc. $C_{30}H_{32}NiN_2O_6$ (%): C, 62.64; H, 5.60; N, 4.87; Ni, 10.20; Found (%): C, 62.70; H, 5.49; N, 4.98; Ni, 10.21.

Complex $Cu(mef)_2 \cdot 2H_2O$: color: green; IR (KBr, ν): 3321 (OH), 3077 (NH), 2910 (CH), 1647 (NH), 1578 (OCO^-), 1506 (NH), 1458 (CH_3), 1393 (OCO^-), 1285 (CH_3), 1188 (CH_3), 1153 (CH), 1067 (CH), 1034 (CH_3), 854 (CH), 746 (CH_3), 680

(MO) cm^{-1} ; Anal. Calc. $C_{30}H_{32}CuN_2O_6$ (%): C, 62.11; H, 5.56; N, 4.83; Cu, 10.95; Found (%): C, 62.08; H, 5.59; N, 4.85; Cu, 10.44.

Complex $Zn(mef)_2 \cdot 2H_2O$: color: white; IR (KBr, ν): 3338 (OH), 3066 (NH), 2858 (CH), 1651 (NH), 1576 (OCO^-), 1506 (NH), 1466 (CH_3), 1388 (OCO^-), 1283 (CH_3), 1183 (CH_3), 1155 (CH), 1069 (CH), 1043 (CH_3), 856 (CH), 748 (CH_3), 677 (MO) cm^{-1} ; Anal. Calc. $C_{30}H_{32}ZnN_2O_6$ (%): C, 61.92; H, 5.54; N, 4.81; Zn, 11.23; Found (%): C, 61.88; H, 5.50; N, 4.88; Zn, 11.25.

Complex $Cd(mef)_2 \cdot 2H_2O$: color: white; IR (KBr, ν): 3312 (OH), 3067 (NH), 2858 (CH), 1651 (NH), 1576 (OCO^-), 1499 (NH), 1452 (CH_3), 1396 (OCO^-), 1283 (CH_3), 1190 (CH_3), 1159 (CH), 1043 (CH_3), 862 (CH), 750 (CH_3), 679 (MO) cm^{-1} ; Anal. Calc. $C_{30}H_{32}CdN_2O_6$ (%): C, 57.29; H, 5.13; N, 4.45; Cd, 17.86; Found (%): C, 57.30; H, 5.15; N, 4.53; Cd, 17.90.

2.3. Measurements. The chemical compositions of all complexes were defined by the elemental analysis followed by the atomic absorption spectrometry. Hydrogen, carbon, and nitrogen contents were measured with the Vario EL III Elemental Analyzer. The metal content was determined in samples mineralized using the Anton Paar Multiwave 3000 closed system instrument. The mixture of concentrated HNO_3 (6 mL) and HCl (2 mL) was applied. Metal concentrations were measured by the FAAS with the GBC Scientific Equipment 932 plus spectrometer.

IR spectra were recorded on FTIR-8501 Shimadzu spectrophotometer over $4000-400 \text{ cm}^{-1}$ range using KBr pellets. The thermal stabilities of complexes were studied by means of TGA techniques. The measurements were made with the Netzsch, TG 209 apparatus, and Q-1500 Derivatograph. Samples ($1 \cdot 10^{-2} \text{ g}$) were heated (in ceramic crucibles) up to 1000°C , at a heating rate $10^\circ\text{C} \cdot \text{min}^{-1}$ in air atmosphere. The analysis of solid decomposition products was performed using TG and DTG curves and supported by the X-ray diffractograms (Siemens D-5000 diffractometer, graphite monochromatized CuK_α radiation) of sinters, obtained by heating the complex samples up to temperatures defined from TG curves. A coupled TG-MS system was applied for analysis of volatile products of thermal decomposition and fragmentation processes. Data were processed using online connected computer system with commercial software (Derivatograph TG/DTA-SETSIS-16/18, coupled to a Mass Spectrometer QMS-422 model ThermoStart from Balzers); platinum crucible, mass sample: 4–6 mg. Dynamic measurements were carried out in argon atmosphere (at a flow rate $20 \text{ mL} \cdot \text{min}^{-1}$) with a heating rate $10^\circ\text{C} \cdot \text{min}^{-1}$ and an ion source temperature of ca. 150°C using 70 eV electron impact ionization. The TG-FTIR measurements were carried out in ceramic crucibles at flowing argon atmosphere ($20 \text{ mL} \cdot \text{min}^{-1}$) using the Netzsch TG 209 apparatus coupled with Bruker FTIR spectrophotometer. The samples were heated up to 1000°C at a heating rate $10^\circ\text{C} \cdot \text{min}^{-1}$. Molar conductivity (Λ_M) of all synthesized compounds was measured in $1 \cdot 10^{-3} \text{ mol} \cdot \text{L}^{-1}$ solutions of MeOH, DMSO, and DMF, according to procedure as described in [24].

TABLE 1: Molar conductivity of complexes $\Lambda_M/\Omega^{-1} \text{ cm}^2 \cdot \text{mol}^{-1}$ for 0,001 mol·L⁻¹ solutions in MeOH, DMF, and DMSO at 25°C.

Complex	Λ_M [$\Omega^{-1} \text{ cm}^2 \text{ mol}^{-1}$]		
	MeOH	DMF	DMSO
Mn(mef) ₂ ·3H ₂ O	45.20	35.70	16.90
Co(mef) ₂ ·2H ₂ O	11.23	13.03	3.07
Ni(mef) ₂ ·2H ₂ O	17.07	20.05	7.09
Cu(mef) ₂ ·2H ₂ O	12.05	13.15	4.27
Zn(mef) ₂ ·2H ₂ O	21.0	28.11	3.17
Cd(mef) ₂ ·2H ₂ O	18.18	24.34	4.55

3. Results and Discussion

The empirical formulae of complexes showing number of water molecules and molar conductivities are presented in Table 1. All synthesized solid complexes are stable in air. They are practically insoluble in water, but on the contrary quite soluble in polar organic solvents (e.g., EtOH, MeOH). Analysis of X-ray powder diffraction data reveals high level of crystallinity and proves that neither pair of investigated compounds is isostructural. The molar conductivity data clearly indicate that all complexes in MeOH and DMSO as well as Co(II), Ni(II), and Cu(II) compounds in DMF are non-electrolytes. On the other hand, molar conductivities for Mn(mef)₂·3H₂O in MeOH and DMF and Zn(mef)₂·2H₂O and Cd(mef)₂·2H₂O point out that solutions of these compounds according to the Geary criterion [25] are intermediates between those of nonelectrolytes and 1:1 electrolytes.

3.1. FTIR Spectra. The IR spectra of all complexes exhibit a broad absorption band in the water stretching region (3300–3600 cm⁻¹). Additionally, bands related to the water bending vibrations are observed (1615–1620 cm⁻¹). In all spectra the valence vibrations of monodissociated carboxylic group are not observed. On the contrary, asymmetric (1575–1578 cm⁻¹) and symmetric (1386–1394 cm⁻¹) vibration of dissociated OCO⁻ group are clearly observed (Table 2). These bands are affected by the coordination of mefenamic ligand to metal ions. The separation $\Delta\nu = \nu_{\text{as}}(\text{OCO}) - \nu_{\text{s}}(\text{OCO})$ and the direction of the shifts of these bands in comparison to those values of sodium salt characterized the nature of the metal–carboxylate bonds. The bathochromic shifts of asymmetric (ν_{as}) and hypsochromic shifts of symmetric (ν_{s}) frequencies are also observed. The magnitude of separation and the bands direction show that carboxylate group of mefenamic ligand coordinated in bidentate chelate mode [26].

Apart from carboxylate group the mefenamic anion has amine group, available for coordination. The NH deformation vibrations in the IR spectra of mefenamic acid are very close to those observed in the IR spectra of its complexes. That indicates that the NH group does not participate directly in coordination.

3.2. Thermal Analysis. The data obtained from TG, DTG, and DTA curves supported by chemical and X-ray diffraction

TABLE 2: Principal IR bands (cm⁻¹) for carboxylate group in investigated complexes.

Compound	ν_{asym}	ν_{sym}	$\Delta\nu = \nu_{\text{asym}} - \nu_{\text{sym}}$
Na(mef)	1580,0	1380,0	200,0
Mn(mef) ₂ ·3H ₂ O	1577,7	1393,6	184,1
Co(mef) ₂ ·2H ₂ O	1577,7	1392,5	185,2
Ni(mef) ₂ ·2H ₂ O	1577,7	1390,6	187,1
Cu(mef) ₂ ·2H ₂ O	1577,7	1392,5	185,2
Zn(mef) ₂ ·2H ₂ O	1575,7	1386,7	189,0
Cd(mef) ₂ ·2H ₂ O	1575,7	1396,4	178,7

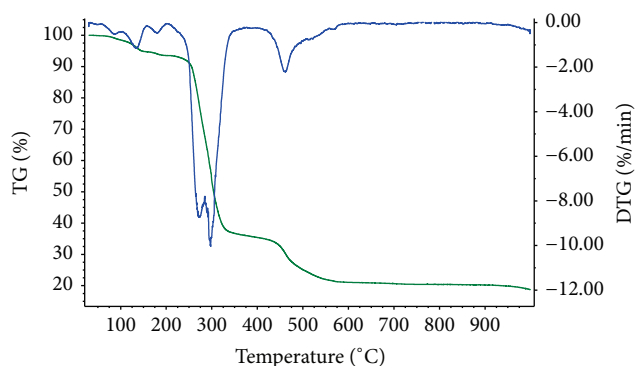


FIGURE 2: Thermoanalytical curves of Cd(mef)₂·2H₂O in air, sample mass 7,407 mg.

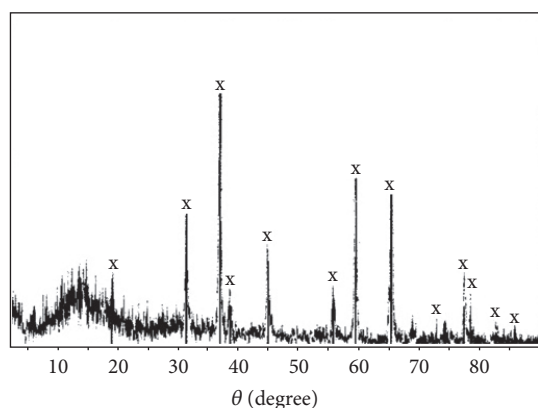
pattern investigations are collected in Table 3. The thermal decomposition curves of Cd(mef)₂·2H₂O are shown on Figure 2. The thermal decomposition of the complexes is a multi-stages process. All compounds started to decompose by dehydration accompanied by the endothermic effect. Majority of complexes lose their water molecules in one step. Only for Co(II) and Zn(II) complexes water elimination is two-stage transformation. Thermolyses of these complexes are quite similar. The two-stage dehydration (60–110°C, 130–240°C and 100–160°C, 160–190°C for Co(II) and Zn(II) compound, respectively) is followed by organic ligand thermodestruction and metal carbonate formation. Further heating leads to metal oxides: ZnO and CoO. The latter is obtained via Co₃O₄ intermediate. In the terminal step of pyrolysis the DTA curve exhibits exoeffects. Formation of oxides was confirmed by the powder X-ray diffraction technique (Figure 3).

Mn(mef)₂·3H₂O and Cu(mef)₂·2H₂O decompose in a similar way. One-step dehydration takes place at 60–240°C and 100–180°C for Mn(II) and Cu(II) complex, respectively. Further increase of temperature results in high mass loss (ca. 80%) caused by mefenamic ligand decomposition and Mn₃O₄ (via Mn₂O₃) and CuO formation. The lowest thermal stability was determined for Ni(II) complex. Its decomposition starts at 50°C with 6,5% mass loss related to water molecules elimination. In the following step, the anhydrous compound decomposes (190–460°C) to NiCO₃. This step is represented as two distinct exothermic peaks at 340°C and 430°C on the DTA curve. Further heating leads to formation of intermediate equimolar mixture of NiO and Ni, which

TABLE 3: Thermal decomposition data of complexes in air.

Compounds	Ranges of decomp., °C	DTA peaks, °C	Mass loss, %		Intermediate and final solid products
			Found	Calc.	
Mn(mef) ₂ ·3H ₂ O	60–240	120 endo	9.0	9.17	Mn(mef) ₂
	240–740	320,600 exo	78.0	77.68	Mn ₂ O ₃
	740–900	860 exo	1.0	1.80	Mn ₃ O ₄
Co(mef) ₂ ·2H ₂ O	60–110	100 endo	3.0	3.13	Co(mef) ₂ ·H ₂ O
	130–240	-	3.0	3.13	Co(mef) ₂
	250–520	340 endo 470 exo	73.0	73.07	CoCO ₃
	530–660	570 exo	7.0	6.72	Co ₃ O ₄
	>900	920 exo	1.0	0.93	CoO
Ni(mef) ₂ ·2H ₂ O	50–180	80 endo	6.5	6.30	Ni(mef) ₂
	190–460	340, 430 exo	73.0	73.10	NiCO ₃
	460–550	490 exo	8.5	9.0	NiO+Ni
	550–750	570 exo	1.5 ^[a]	1.39 ^[a]	NiO
Cu(mef) ₂ ·2H ₂ O	100–180	150 endo	6.5	6.66	Cu(mef) ₂
	190–840	550, 640 exo	80.0	80.08	CuO
Zn(mef) ₂ ·2H ₂ O	100–160	130 endo	3.0	3.10	Zn(mef) ₂ ·H ₂ O
	160–190	180 endo	3.0	3.10	Zn(mef) ₂
	200–490	420 exo	72.0	72.26	ZnCO ₃
	490–640	510 endo, 580 exo	8.0	7.56	ZnO
Cd(mef) ₂ ·2H ₂ O	110–160	150 endo	6.0	5.73	Cd(mef) ₂
	210–380	300 endo, 340 exo	67.0	66.86	CdCO ₃
	470–760	550 exo	7.0	6.59	CdO

^[a]Mass increase on TG curve.



x: CO₃O₄

FIGURE 3: X-ray powder diffraction patterns of decomposition products of Co(mef)₂·2H₂O heated up to 660°C.

subsequently is fully oxidized to nickel oxide (mass increase on the TG curve). Presence of NiO was confirmed by powder X-ray diffraction of sinters prepared by heating compound to 750°C. The highest thermal stability is shown by Cd(II) complex. Its pyrolysis pattern closely resembles that of Ni(II)

complex. Dehydration is single-step process and started at 110°C. The next mass loss (210–380°C) as observed on TG curve corresponds to destruction of organic ligand and leads to formation of CdCO₃. The latter is associated with endo- and exothermic effects as represented by two distinct DTA peaks at 300 and 340°C, respectively. Further weight loss is observed at 470–760°C and results from the CdO formation (maximum on DTA curves at 550°C).

3.3. *TG-MS Measurement.* Conventional thermoanalytic studies such as TG/DTA often do not allow for unequivocal identification of gaseous products. For this reason, the TG/MS techniques were employed to characterize products of dynamic decomposition and fragmentation of Mn(mef)₂·3H₂O and Co(mef)₂·2H₂O. The determination was carried out under an argon atmosphere. The *m/z* values are given for ¹H, ¹²C, ¹⁴N, and ¹⁶O. Figure 4 presents some profiles of ion current detected by mass spectrometer as a function of time for Co(II) complex. MS peaks of ion fragments corresponding to H₂⁺, C⁺, CH₃⁺, OH⁺, H₂O⁺, C₂H₂⁺, HCN⁺, N₂⁺, C₂H₅⁺, NO⁺, CO₂⁺, ¹³C¹⁶O₂⁺, ¹³C¹⁶O¹⁸O⁺ (*m/z* = 1, 12, 15, 17, 18, 26, 27, 28, 29, 30, 44, 45, 46) are monitored. Recorded data clearly indicated that all investigated complexes decompose progressively. For Mn(II) complex maxima

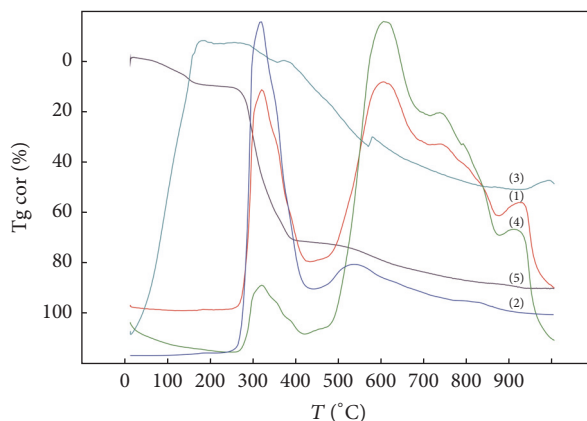


FIGURE 4: TG and corresponding MS analysis of $\text{Co(mef)}_2 \cdot 2\text{H}_2\text{O}$ (where: (1) $m/z = 12$; (2) $m/z = 15$; (3) $m/z = 18$; (4) $m/z = 44$; (5) TG).

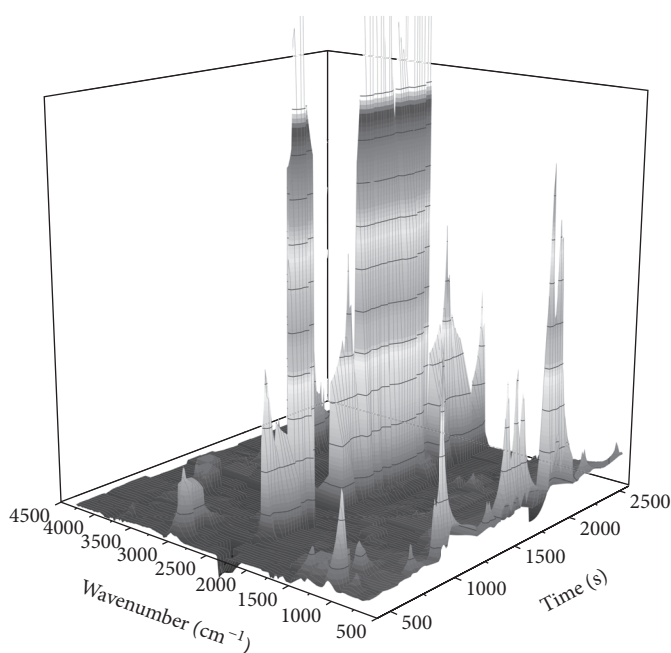


FIGURE 5: The stacked plot TG-FTIR spectra of the evolved gases for $\text{Cd(mef)}_2 \cdot 2\text{H}_2\text{O}$.

of ion current intensities were observed for temperature ranges 120–280°C, 270–450°C, and 600–900°C.

The peaks from H_2O^+ and H_2^+ observed at 110 and 120°C are related to dehydration of complex. Subsequently, fragmentation of organic ligand occurred within the 120–180°C temperature range. The following molecular ions were detected (respective temperature maxima are given in parentheses): C_3H_7^+ (160°C), CH_3^+ (150°C), C_2H_2^+ (170°C), C_2H_5^+ (165°C), C^+ (210°C), CO_2^+ (215°C), $^{13}\text{C}^{16}\text{O}_2^+$ (180°), (HCN^+ , N_2^+). Three major temperature ranges of gaseous products emissions 120–230°C, 230–400°C, and 500–900°C were recorded for $\text{Co(mef)}_2 \cdot 2\text{H}_2\text{O}$. In the first area, CH_3^+ , C_2H_5^+ , C_2H_2^+ ions were detected (all maxima at 160°C). The second is related to C^+ , CO_2^+ including combination of isotopes (ca. 300°C) while the third range corresponds to C^+ , CH_3^+ , C_2H_5^+ , and CO_2^+ ions.

3.4. TG-FTIR Measurement. The coupled TG-FTIR technique was applied to $\text{Cd(mef)}_2 \cdot 2\text{H}_2\text{O}$, $\text{Cu(mef)}_2 \cdot 2\text{H}_2\text{O}$, and $\text{Zn(mef)}_2 \cdot 2\text{H}_2\text{O}$ complexes. All experiments were performed in argon atmosphere. The IR spectra were recorded using the Gramm-Schmidt curves. The respective stacked plot as registered for $\text{Cd(mef)}_2 \cdot 2\text{H}_2\text{O}$ is given in Figure 5.

Analysis of IR spectra of gases evolved during the thermal decomposition indicates that pyrolysis schemes of all investigated complexes are similar and closely related to those recorded in air atmosphere. All spectra clearly confirm that the thermal decomposition begins from the dehydration process. On the TG curve in range 100–160°C for $\text{Cd(mef)}_2 \cdot 2\text{H}_2\text{O}$ and $\text{Cu(mef)}_2 \cdot 2\text{H}_2\text{O}$ and 100–190°C for $\text{Zn(mef)}_2 \cdot 2\text{H}_2\text{O}$ ca. 6% mass losses connected with water losing were observed. The IR spectra which recorded up to 120°C for Cd(II) and Cu(II) complexes and up to 150°C for Zn(II) complex show bands in the wavenumbers 3750–3500

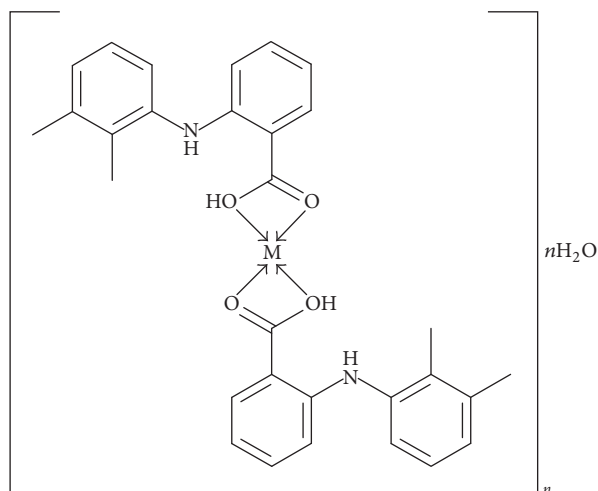


FIGURE 6: Proposed formula of the mefenamic-metal complexes.

and $1750\text{--}1400\text{ cm}^{-1}$ corresponding to stretching and deformation vibrations of liberating water molecules. Anhydrous complexes are stable up to about 170°C which is confirmed by the lack of IR spectra of gaseous products. Further heating leads to organic ligand degradation indicated by a significant mass loss observed on the TG curve. The spectra recorded at 260°C contain bands in frequencies ranging $3000\text{--}2600\text{ cm}^{-1}$ (assigned to the stretching vibrations of the CH bond from the CH_3 and CH_2 groups); $1450\text{--}1350\text{ cm}^{-1}$ (corresponding to bending vibrations of the CH in the CH_3 and CH_2 groups); $1225\text{--}1000\text{ cm}^{-1}$ and $900\text{--}720\text{ cm}^{-1}$ (from bending vibration of CH in aromatic ring). Additionally, this spectrum shows the trace of water molecules in split of organic ligand destruction (tied in with NH vibration). Spectra which recorded up to 290°C contain the same patterns as described above augmented by additional bands (in the range $2500\text{--}2250\text{ cm}^{-1}$ and $750\text{--}650\text{ cm}^{-1}$) corresponding to CO_2 vibrations and trace CO oscillations ($2250\text{--}2050\text{ cm}^{-1}$). Heating the sample above 450°C resulted in rising intensity of bands related to carbon oxides while in the same time decreasing those of water and complete absence of aromatic ring vibrations.

4. Conclusions

All investigated complexes have been obtained as crystalline hydrates. Majority of synthesized compounds in MeOH, DMSO, and DMF solutions do not dissociate or dissociate only in a very limited degree. IR spectra firmly confirmed that mefenamic ligands are directly coordinated to metal ions only through carboxylate group, in a bidentate chelate mode. According to the chemical, spectroscopic, and thermal data, we have proposed the formula of obtained complexes (Figure 6).

All compounds decompose progressively starting with dehydration at the temperature range $60\text{--}150^\circ\text{C}$. Anhydrous compounds are stable up to almost 170°C . The most temperature persistence is Cd(II) complex, while the least one is the Ni(II) compound. Results of the TG-MS and TG-FTIR investigations correlate closely with those obtained by the

TG-DTG system. The differences are related to final products and paths of dehydration.

Conflicts of Interest

The authors declare that they have no conflicts of interest.

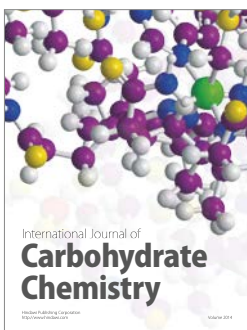
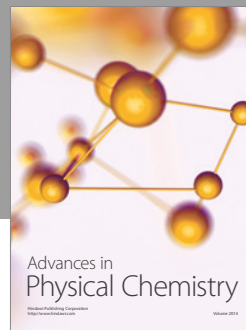
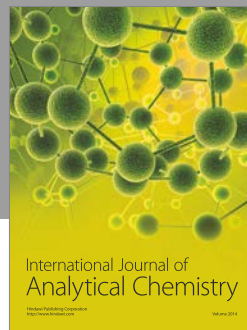
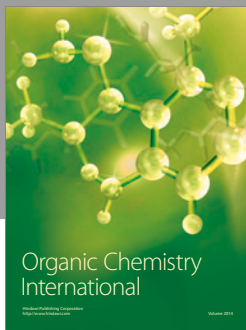
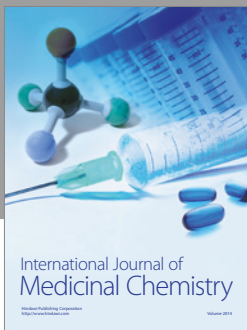
Supplementary Materials

The supplementary material includes the TG/DTG/DTA, TG-MS, and TG-FTIR plots for synthesized complexes. Figure 1A. TG/DTG/DTA curves of $\text{Mn}(\text{mef})_2 \cdot 3\text{H}_2\text{O}$. Figure 2A. TG/DTG/DTA curves of $\text{Co}(\text{mef})_2 \cdot 2\text{H}_2\text{O}$. Figure 3A. TG/DTG/DTA curves of $\text{Ni}(\text{mef})_2 \cdot 2\text{H}_2\text{O}$. Figure 4A. TG/DTG/DTA curves of $\text{Cu}(\text{mef})_2 \cdot 2\text{H}_2\text{O}$. Figure 5A. TG/DTG/DTA curves of $\text{Zn}(\text{mef})_2 \cdot 2\text{H}_2\text{O}$. Figure 6A. TG/DTG/DTA curves of $\text{Cd}(\text{mef})_2 \cdot 2\text{H}_2\text{O}$. Figure 7A. TG and corresponding MS analysis of $\text{Mn}(\text{mef})_2 \cdot 3\text{H}_2\text{O}$ (where: (1) $m/z = 12$; (2) $m/z = 15$; (3) $m/z = 18$; (4) $m/z = 44$; (5) TG). Figure 8A. The stacked plot TG-FTIR spectra of the evolved gases for $\text{Cu}(\text{mef})_2 \cdot 2\text{H}_2\text{O}$. Figure 9A. The stacked plot TG-FTIR spectra of the evolved gases for $\text{Zn}(\text{mef})_2 \cdot 2\text{H}_2\text{O}$. (Supplementary Materials)

References

- [1] J. R. Vane and R. M. Botting, "Mechanism of action of nonsteroidal anti-inflammatory drugs," *American Journal of Medicine*, vol. 104, no. 3 A, 1998.
- [2] J. R. Vane, "Inhibition of prostaglandin synthesis as a mechanism of action for aspirin-like drugs," *Nature: New biology*, vol. 231, no. 25, pp. 232–235, 1971.
- [3] F. A. Aly, S. A. Al-Tamimi, and A. A. Alwarthan, "Determination of flufenamic acid and mefenamic acid in pharmaceutical preparations and biological fluids using flow injection analysis with tris(2,2'-bipyridyl)ruthenium(II) chemiluminescence detection," *Analytica Chimica Acta*, vol. 416, no. 1, pp. 87–96, 2000.
- [4] N. Cimolai, "The potential and promise of mefenamic acid," *Expert Review of Clinical Pharmacology*, vol. 6, no. 3, pp. 289–305, 2013.
- [5] S. Cesur and S. Gokbel, "Crystallization of mefenamic acid and polymorphs," *Crystal Research and Technology*, vol. 43, no. 7, pp. 720–728, 2008.
- [6] I. H. Sahin, M. M. Hassan, and C. R. Garrett, "Impact of non-steroidal anti-inflammatory drugs on gastrointestinal cancers: Current state-of-the science," *Cancer Letters*, vol. 345, no. 2, pp. 249–257, 2014.
- [7] P. Ghanghas, S. Jain, C. Rana, and S. N. Sanyal, "Chemopreventive action of non-steroidal anti-inflammatory drugs on the inflammatory pathways in colon cancer," *Biomedicine & Pharmacotherapy*, vol. 78, pp. 239–247, 2016.
- [8] I. Jasya and K. Hideo, Jpn. Patent No. 59-175220, 1986.
- [9] K. Hirojuki, J. Mitihiro, and S. Enuhisa, Jpn. Patent No. 69-134541, 1989.
- [10] F. Dimiza, S. Fountoulaki, A. N. Papadopoulos et al., "Non-steroidal antiinflammatory drug-copper(II) complexes: Structure and biological perspectives," *Dalton Transactions*, vol. 40, no. 34, pp. 8555–8568, 2011.

- [11] S. B. Etcheverry, D. A. Barrio, A. M. Cortizo, and P. A. M. Williams, "Three new vanadyl(IV) complexes with non-steroidal anti-inflammatory drugs (Ibuprofen, Naproxen and Tolmetin). Bioactivity on osteoblast-like cells in culture," *Journal of Inorganic Biochemistry*, vol. 88, no. 1, pp. 94–100, 2002.
- [12] C. Núñez, A. Fernández-Lodeiro, J. Fernández-Lodeiro, J. Carballo, J. L. Capelo, and C. Lodeiro, "Synthesis, spectroscopic studies and in vitro antibacterial activity of Ibuprofen and its derived metal complexes," *Inorganic Chemistry Communications*, vol. 45, pp. 61–65, 2014.
- [13] J. Feng, X. Du, H. Liu et al., "Manganese-mefenamic acid complexes exhibit high lipoxygenase inhibitory activity," *Dalton Transactions*, vol. 43, no. 28, pp. 10930–10939, 2014.
- [14] X. Totta, A. A. Papadopoulou, A. G. Hatzidimitriou, A. Papadopoulos, and G. Psomas, "Synthesis, structure and biological activity of nickel(II) complexes with mefenamato and nitrogen-donor ligands," *Journal of Inorganic Biochemistry*, vol. 145, pp. 79–93, 2015.
- [15] A. Ashraf, W. A. Siddiqui, J. Akbar et al., "Metal complexes of benzimidazole derived sulfonamide: Synthesis, molecular structures and antimicrobial activity," *Inorganica Chimica Acta*, vol. 443, pp. 179–185, 2016.
- [16] S. Ramzan, S. Saleem, B. Mirza, S. Ali, F. Ahmed, and S. Shahzadi, "Synthesis, characterization, and biological activity of transition metals complexes with mefenamic acid (NSAIDs)," *Russian Journal of General Chemistry*, vol. 85, no. 7, pp. 1745–1751, 2015.
- [17] C. T. Dillon, T. W. Hambley, B. J. Kennedy et al., "Gastrointestinal toxicity, antiinflammatory activity, and superoxide dismutase activity of copper and zinc complexes of the antiinflammatory drug indomethacin," *Chemical Research in Toxicology*, vol. 16, no. 1, pp. 28–37, 2003.
- [18] K. Kafarska, D. Czakis-Sulikowska, and W. M. Wolf, "Novel Co(II) and Cd(II) complexes with non-steroidal anti-inflammatory drugs: Synthesis, properties and thermal investigation," *Journal of Thermal Analysis and Calorimetry*, vol. 96, no. 2, pp. 617–621, 2009.
- [19] R. P. Sharma, S. Singh, A. Singh, and V. Ferretti, "Spectra-structure relationship: Synthesis, characterization of copper(II) complexes with ibuprofenate, o-methoxybenzoate, p-ethoxybenzoate and single crystal X-ray structure determination of $[\text{trans-Cu}(\text{en})_2(\text{H}_2\text{O})_2](\text{L})_2$ where en = ethylenediamine, L = o-methoxybenzoate/p-ethoxybenzoate," *Journal of Molecular Structure*, vol. 918, no. 1-3, pp. 188–193, 2009.
- [20] C. Dendrinou-Samara, D. P. Kessissoglou, G. E. Manoussakis, D. Mentzafos, and A. Terzis, "Copper(II) complexes with anti-inflammatory drugs as ligands. Molecular and crystal structures of bis(dimethyl sulphoxide)tetrakis(6-methoxy- α -methyl-2-naphthaleneacetato)dicopper(II) and bis(dimethyl sulphoxide)tetrakis[1-methyl-5-(p-toluoyl)-1H-pyrrole-2-acetato]dicopper(II)," *Journal of the Chemical Society, Dalton Transactions*, no. 3, pp. 959–965, 1990.
- [21] W. Brzyska and W. Ożga, "Preparation and properties of rare earth element complexes with mephenamic acid," *Polish Journal of Chemistry*, vol. 67, p. 619, 1993.
- [22] A. Topaçli and S. Ide, "Molecular structures of metal complexes with mefenamic acid," *Journal of Pharmaceutical and Biomedical Analysis*, vol. 21, no. 5, pp. 975–982, 1999.
- [23] D. Kovala-Demertzi, V. Dokorou, Z. Ciunik, N. Kourkoumelis, and M. A. Demertzis, "Organotin mefenamic complexes-preparations, spectroscopic studies and crystal structure of a triphenyltin ester of mefenamic acid: Novel anti-tuberculosis agents," *Applied Organometallic Chemistry*, vol. 16, no. 7, pp. 360–368, 2002.
- [24] D. Czakis-Sulikowska, A. Malinowska, and K. Kafarska, "Complexes of Mn(II), Cu(II) and Cd(II) with bipyridine isomers and lactates," *Polish Journal of Chemistry*, vol. 80, no. 12, pp. 1945–1958, 2006.
- [25] W. J. Geary, "The use of conductivity measurements in organic solvents for the characterisation of coordination compounds," *Coordination Chemistry Reviews*, vol. 7, no. 1, pp. 81–122, 1971.
- [26] K. Nakamoto, *Infrared and Raman Spectra of Inorganic and Coordination Compounds*, John Wiley & Sons, Inc., New York, NY, USA, 2009.



Hindawi

Submit your manuscripts at
<https://www.hindawi.com>

